$tRNA^{His}$ 5-methylcytidine levels increase in response to several growth arrest conditions in *Saccharomyces cerevisiae*

MELANIE A. PRESTON,[1] SONIA D'SILVA, YOSHIKO KON, and ERIC M. PHIZICKY[2]

Department of Biochemistry and Biophysics and Center for RNA Biology, University of Rochester School of Medicine, Rochester, New York 14642, USA

ABSTRACT

tRNAs are highly modified, each with a unique set of modifications. Several reports suggest that tRNAs are hypomodified or, in some cases, hypermodified under different growth conditions and in certain cancers. We previously demonstrated that yeast strains depleted of $tRNA^{His}$ guanylyltransferase accumulate uncharged $tRNA^{His}$ lacking the G_{-1} residue and subsequently accumulate additional 5-methylcytidine (m^5C) at residues C_{48} and C_{50} of $tRNA^{His}$, due to the activity of the m^5C-methyltransferase Trm4. We show here that the increase in $tRNA^{His}$ m^5C levels does not require loss of Thg1, loss of G_{-1} of $tRNA^{His}$, or cell death but is associated with growth arrest following different stress conditions. We find substantially increased $tRNA^{His}$ m^5C levels after temperature-sensitive strains are grown at nonpermissive temperature, and after wild-type strains are grown to stationary phase, starved for required amino acids, or treated with rapamycin. We observe more modest accumulations of m^5C in $tRNA^{His}$ after starvation for glucose and after starvation for uracil. In virtually all cases examined, the additional m^5C on $tRNA^{His}$ occurs while cells are fully viable, and the increase is neither due to the *GCN4* pathway, nor to increased Trm4 levels. Moreover, the increased m^5C appears specific to $tRNA^{His}$, as $tRNA^{Val(AAC)}$ and $tRNA^{Gly(GCC)}$ have much reduced additional m^5C during these growth arrest conditions, although they also have C_{48} and C_{50} and are capable of having increased m^5C levels. Thus, $tRNA^{His}$ m^5C levels are unusually responsive to yeast growth conditions, although the significance of this additional m^5C remains unclear.

Keywords: tRNA(His); tRNA modifications; 5-methylcytidine; Trm4; cellular stress

INTRODUCTION

During maturation, tRNA molecules are extensively processed and highly modified with a unique set of post-transcriptional modifications. In *Saccharomyces cerevisiae*, ~13 nt are modified in each tRNA, and there are 25 unique tRNA modifications that have been found at 36 positions on the tRNA (Phizicky and Hopper 2010). These post-transcriptional modifications are highly conserved in different organisms, underscoring their importance. Many tRNA modifications near the anti-codon have important roles in decoding mRNA (Agris et al. 2007), as evidenced by lethality or slow growth phenotypes (Phizicky and Hopper 2010). For example, loss of 2′-O-methylation at positions 32 and 34 or loss of either m^1G or t^6A at position 37 results in slow growth (Bjork et al. 2001; Pintard et al. 2002; El Yacoubi et al. 2009; Guy et al. 2012). In addition, a number of modifications in the tRNA body have important roles in stabilizing tRNA (Kadaba et al. 2004; Alexandrov et al. 2006; Kadaba et al. 2006; Chernyakov et al. 2008b; Phizicky and Hopper 2010; Whipple et al. 2011). However, the precise roles of many modifications are not yet known in detail and are still under investigation.

Although it has been generally assumed that modifications made to tRNAs are constitutively added at similar levels, a number of reports have described altered tRNA modification levels under various conditions in different organisms. *Bacillus subtilis* tRNAs were reported to be hypomethylated during log phase growth (Singhal and Vold 1976), and *Bacillus stearothermophilus* tRNAs have higher 2′-O-methylation levels at 70°C than at 50°C (Agris et al. 1973). Similarly, several types of cancer cell lines have reduced yW (wybutosine) modification of $tRNA^{Phe}$ (Grunberger et al. 1975; Mushinski and Marini 1979, 1983; Kuchino et al. 1982; Grunberger et al. 1983), and $tRNA^{Phe}$ species from a hepatoma and a breast carcinoma have an unexpected additional 1-methylguanosine (m^1G) modification, as well as additional dihydrouridine and 5-methylcytidine (m^5C) (Kuchino and Borek 1978). In addition, human and murine hepatoma cells have reduced levels of queosine in their $tRNA^{Asp}$ (Kuchino et al. 1981; Randerath et al. 1984; Pathak et al. 2005), while in *Drosophila*, queosine levels of several tRNAs increase with

[1]**Present address:** Department of Biochemistry, University of Wisconsin, Madison, WI 53706, USA

[2]**Corresponding author**

E-mail eric_phizicky@urmc.rochester.edu

Article published online ahead of print. Article and publication date are at http://www.rnajournal.org/cgi/doi/10.1261/rna.035808.112.

age and with the percentage of yeast in the diet (Hosbach and Kubli 1979; Owenby et al. 1979).

Emerging data also suggest growth-dependent changes in tRNA modification levels in the yeast *Saccharomyces cerevisiae*. Mitochondrial $tRNA^{Lys(UUU)}$ has reduced 2-thiolation following growth at elevated temperature (Kamenski et al. 2007). In addition, it was recently reported that oxidative stress mediated by hydrogen peroxide results in increased levels of m^5C, 2′-O-methylcytidine (Cm), and 2,2-dimethylguanosine (m^2_2G) levels and that a number of other modifications are affected by treatment with several chemicals that induce cellular stress (Chan et al. 2010, 2012).

We previously reported that depletion of the essential $tRNA^{His}$ guanylyltransferase Thg1 results in the loss of G_{-1} from $tRNA^{His}$, with concomitant accumulation of deacylated $tRNA^{His}$ and the subsequent accumulation of additional m^5C on $tRNA^{His}$ ~8 h after the loss of G_{-1} (Gu et al. 2005). The additional m^5C occurs at residues C_{48} and C_{50} (~0.5 mol/mol tRNA at each position) (Gu et al. 2005), adjacent to the known m^5C_{49} modification, and appears to be due to Trm4 methyltransferase, which catalyzes formation of m^5C at C_{34}, C_{40}, C_{48}, and C_{49} in all substrate tRNAs in yeast (Motorin and Grosjean 1999). Interestingly, the additional m^5C that accumulates following Thg1 depletion was not found on $tRNA^{Gly(GCC)}$, which also has cytidines at these positions, and $tRNA^{His}$ was observed to accumulate in the nucleus during Thg1 depletion (Gu et al. 2005), presumably by retrograde transport of cytoplasmic tRNA to the nucleus (Shaheen and Hopper 2005; Takano et al. 2005). At the time, we speculated that the additional m^5C found in $tRNA^{His}$ from Thg1-depleted cells might be due to the increased availability of deacylated $tRNA^{His}$ to Trm4, which is localized to the nucleus (Wu et al. 1998), or possibly due to a regulatory response from the uncharged $tRNA^{His}$ as the cells arrested growth due to loss of Thg1 (Gu et al. 2005). Alternatively, the lack of the G_{-1} modification on $tRNA^{His}$ might trigger the accumulation of m^5C, much as *Thermus thermophilus* cells lacking either m^7G_{46} or ψ_{55} have altered modifications under certain conditions (Tomikawa et al. 2010; Ishida et al. 2011).

In this work, we explore the conditions in which $tRNA^{His}$ can be modified with additional m^5C. We show that m^5C accumulates in $tRNA^{His}$ under a variety of conditions in which growth is arrested and that this accumulation is not associated with cell death. Although several conditions examined involve nutrient deprivation, the *GCN4* pathway is not responsible for the additional m^5C. However, the target of rapamycin (TOR) pathway may play a role in the m^5C response, since rapamycin treatment results in an increase in $tRNA^{His}$ m^5C levels. Remarkably, we also show that this additional m^5C is specific to $tRNA^{His}$, relative to two other tRNAs with cytidine residues at the same positions, which are capable of being overmodified with m^5C in vivo. We conclude that m^5C modification of $tRNA^{His}$ is unusually sensitive to yeast growth conditions, although the cellular function of this phenomenon remains unclear.

RESULTS

m^5C levels are increased in $tRNA^{His}$ from *thg1*^{ts} strains but not from a *thg1*-Δ strain

Our initial goal was to explore the cause of additional m^5C on $tRNA^{His}$ observed following depletion of Thg1 (Gu et al. 2005), which adds G_{-1} to the 5′ end of $tRNA^{His}$ (Gu et al. 2003). The secondary structure and modifications of $tRNA^{His}$ are depicted in Figure 1A. The m^5C modification (catalyzed by Trm4) is clearly resolved from other nucleosides by reverse-phase HPLC analysis of $tRNA^{His}$ purified from wild-type and *trm4*-Δ strains (Fig. 1B). Values of nucleoside modifications are quantified from HPLC traces and are expressed as moles of modification per mole of tRNA (mol/mol tRNA).

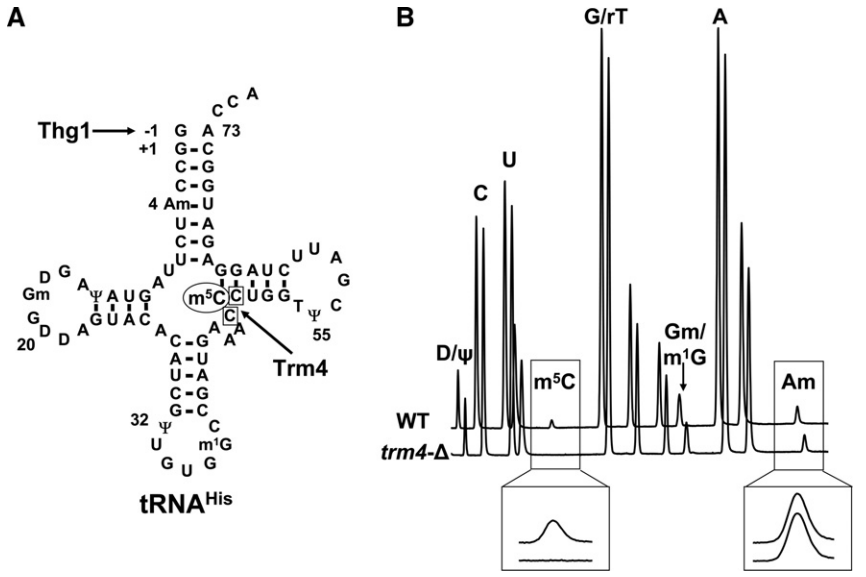

FIGURE 1. Post-transcriptional modifications of mature $tRNA^{His}$. (*A*) Secondary structure of mature *S. cerevisiae* $tRNA^{His}$. Post-transcriptional modifications are indicated. G_{-1} is added to the 5′ end of $tRNA^{His}$ by $tRNA^{His}$ guanylyltransferase (Thg1). Under normal growth conditions, Trm4 methylates position 49 to form 5-methylcytidine (m^5C, circle). When Thg1 is depleted, Trm4 also methylates adjacent cytidines at positions 48 and 50 (squares). (*B*) Representative HPLC traces of $tRNA^{His}$ nucleosides. Wild-type (BY4741) and *trm4*-Δ cells were grown to log phase in SD complete media, and $tRNA^{His}$ was purified, digested with P1 nuclease, phosphatase-treated, and separated by reverse-phase HPLC. *Insets* compare the wild type vs. *trm4*-Δ m^5C peak (*left*), with the Am peak (*right*) as a control.

Based on our previously published data, it seemed plausible that increased levels of m^{5}C upon Thg1 depletion might be due to the loss of the essential Thg1 protein, the consequent loss of the tRNA^{His} G$_{-1}$ residue, and the accumulation of uncharged tRNA^{His} (Gu et al. 2005). To test this, we examined a *thg1*-Δ strain that was viable due to overexpression of tRNA^{His} and the histidyl-tRNA synthetase *HTS1* (Preston and Phizicky 2010). We find that this strain has normal levels of m^{5}C on tRNA^{His} relative to wild type (Table 1, *WT*). Since this *thg1*-Δ strain also has approximately 15-fold more tRNA^{His} than a wild-type strain and the tRNA^{His} is mostly deacylated (Preston and Phizicky 2010), the availability of uncharged tRNA^{His} alone is likely not the cause of additional m^{5}C levels. In support of this conclusion, increasing the amount of available tRNA^{His} by overexpression of tRNA^{His} in a wild-type strain has no effect on tRNA^{His} m^{5}C levels (Table 1). Therefore, it is possible that the addition of m^{5}C to tRNA^{His} is, instead, triggered by growth arrest due to loss of Thg1 function.

To explore the connection between Thg1 depletion-mediated growth arrest and elevated tRNA^{His} m^{5}C levels, we measured m^{5}C levels in tRNA^{His} purified from three different *thg1* temperature-sensitive mutants (Y146H, G172D/L233S, and Y8C) before and after shift to 37°C (Table 1). Growth arrest was apparent by 3 h for the *thg1-Y146H* strain and by 4–5 h for the *thg1-G172D/L233S* and *thg1-Y8C* strains (data not shown). Whereas tRNA^{His} from the wild-type strain and each of the *thg1* mutants have near normal amounts of m^{5}C when grown at 24°C (0.92–1.25 mol/mol tRNA), tRNA^{His} m^{5}C levels increase dramatically to 2.36–2.41 mol/mol tRNA when *thg1* mutants are shifted to 37°C for 7 h. tRNA^{His} from the wild-type strain has normal levels of m^{5}C after the temperature shift, and levels of control modifications (dihydrouridine (D), pseudouridine (ψ), m^{1}G, and Am) remain unchanged in tRNA^{His} isolated from each strain (Table 1; data not shown).

tRNA^{His} m^{5}C levels increase when temperature-sensitive strains are grown at nonpermissive temperature

Based on the data above, the increase in m^{5}C levels could be correlated with lack of growth or with cell death, associated with loss of Thg1 function. To determine if an increase in tRNA^{His} m^{5}C levels is specific to loss of Thg1 function and/or subsequent cell death, we grew a set of temperature-sensitive (ts) strains at permissive or nonpermissive temperatures and analyzed cell viability. We then purified tRNA^{His} and measured modification levels by HPLC analysis. We grew BY4741 (*WT*) and the *thg1-Y146H*^{ts} strain as a control for additional m^{5}C. We also grew three temperature-sensitive strains unrelated to tRNA processing: the *fcp1-1*^{ts} strain, which is defective for transcription by RNA polymerase II at nonpermissive temperature (Kobor et al. 1999), the *abf1-102*^{ts} strain, which has a mutation in a DNA binding protein involved in transcriptional regulation, DNA replication, and DNA repair (Buchman et al. 1988; Reed et al. 1999; Miyake et al. 2004), and the *cdc48-9*^{ts} strain, which has a mutation in an ATPase involved in protein export from the ER to the cytoplasm (Ye et al. 2001). Growth arrest was apparent by 2–3 h for the *fcp1-1*^{ts} strain, by 3–4 h for the *thg1-Y146H*^{ts} strain, by 6–7 h for the *cdc48-9*^{ts} strain, and by over 7 h for the *abf1-102*^{ts} strain (data not shown).

For two of the temperature-sensitive strains grown at 37°C, we observe an increase in m^{5}C levels on tRNA^{His} following growth arrest and without any significant loss of cell viability (Fig. 2; Table 2). Thus, at the 7 h time point at 37°C, the *fcp1-1*^{ts} and *cdc48-9*^{ts} strains are nearly completely viable

TABLE 1. tRNA^{His} modification levels in conditions of reduced Thg1 activity

Strain	2μ plasmid	Temp. (°C)	ψ	m^{5}C
thg1-Δ [*HTS1*]	tRNA^{His}	30[a]	3.03 ± 0.06	0.99 ± 0.04
BY4741 (*WT*)	—	30[b]	2.87 ± 0.08	0.94 ± 0.04
BY4741 (*WT*)	tRNA^{His}	30[a]	3.00 ± 0.03	1.05 ± 0.01
	Vector	30[b]	2.90 ± 0.09	0.95 ± 0.08
THG1 (WT)	—	24[a]	2.91 ± 0.08	0.92 ± 0.03
	—	37[a]	2.97 ± 0.10	1.12 ± 0.02
thg1-Y146H	—	24[c]	2.95 ± 0.11	0.98 ± 0.06
	—	37[c]	3.11 ± 0.04	2.40 ± 0.12[d]
thg1-G172D/L233S	—	24	2.94	0.99
	—	37	3.08	2.41
thg1-Y8C	—	24	3.86	1.25
	—	37	3.24	2.36
Expected mol/mol tRNA			3	1

[a] $n = 4$, mean ± standard deviation.
[b] $n = 5$, mean ± standard deviation.
[c] $n = 3$, mean ± standard deviation.
[d] tRNA^{His} m^{5}C from *thg1-Y146H* 24°C vs. 37°C: Student's *t*-test, $P = 2.1 \times 10^{-4}$.

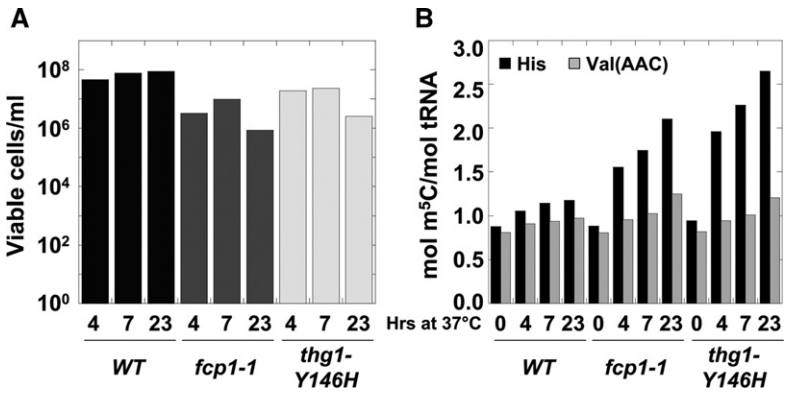

FIGURE 2. Temperature-sensitive strains have additional m^5C on $tRNA^{His}$ when grown at nonpermissive temperature. (*A*) Assessment of viable cell titer following growth at 37°C. (*B*) m^5C levels in $tRNA^{His}$ and $tRNA^{Val(AAC)}$ during growth at 37°C. $tRNA^{His}$ and $tRNA^{Val(AAC)}$ were purified from BY4741, *thg1-Y146H*, and *fcp1-1* strains, and modification levels were measured by HPLC. m^5C levels for $tRNA^{His}$ (black) and $tRNA^{Val(AAC)}$ (gray) during temperature-sensitive strain growth at 37°C were plotted. m^5C values during growth at 24°C were plotted as the 37°C 0-h time point.

(Fig. 2A; Table 2; data not shown) and their $tRNA^{His}$ have 1.75 and 1.51 mol m^5C/mol tRNA, respectively, compared to 0.92 and 0.93 mol/mol tRNA at 24°C (Fig. 2B; Table 2; data not shown). At the same time point after shift to 37°C, $tRNA^{His}$ m^5C levels increase only slightly in the wild-type strain (from 0.92 to 1.12 mol/mol tRNA) and in the *abf1-102*^{ts} mutant (from 0.89 to 1.18 mol/mol tRNA) (data not shown). We ruled out the possibility that the increased $tRNA^{His}$ m^5C levels in the *fcp1-1*^{ts} strain were somehow due to the absence of the G_{-1} residue of $tRNA^{His}$ by direct examination of the 5′ end of $tRNA^{His}$. As expected, there was no change in the G_{-1} status in *fcp1-1*^{ts} and *WT* strains and a marked reduction in G_{-1} of $tRNA^{His}$ from the *thg1-Y146H*^{ts} grown at 37°C (data not shown). Thus, the additional m^5C on $tRNA^{His}$ is unrelated to the G_{-1} addition activity of Thg1, and we conclude that growth arrest, but not cell death, of temperature-sensitive strains results in additional m^5C on $tRNA^{His}$.

We also find evidence that the increased amount of m^5C is specific to $tRNA^{His}$. $tRNA^{Val(AAC)}$, which also normally has unmodified C_{48} and C_{50} residues adjacent to m^5C_{49}, has only marginally increased levels of m^5C 7 h after temperature shift in the *fcp1-1*^{ts} mutant (from 0.81 to 1.03 mol/mol tRNA) and in the *thg1-Y146H*^{ts} mutant (from 0.82 to 1.01 mol/mol tRNA) (Fig. 2B; Table 2).

$tRNA^{His}$ m^5C levels increase in several conditions in which a wild-type strain arrests growth and is still viable

Since the accumulation of m^5C in $tRNA^{His}$ occurs in temperature-sensitive strains following growth arrest, we reasoned that wild-type strains might also have elevated m^5C levels in conditions where the cells stop growing. We, therefore,

TABLE 2. Temperature-sensitive strains grown at nonpermissive temperature have additional m^5C on $tRNA^{His}$

			$tRNA^{His}$				$tRNA^{Val(AAC)}$				
Strain	Temp. (°C)	Time (h)	ψ	m^5C	Gm + m^1G	Am	ψ	m^5C	I	m^1G	Viable cells/mL[g]
BY4741	24	6[a]	2.91 ± 0.08	0.92 ± 0.03	2.04 ± 0.04	0.93 ± 0.04	3.85	0.81	1.19	1.12	9.8×10^6
	37	4	2.97	1.06	2.10	0.94	3.81	0.91	1.25	1.10	4.6×10^7
	37	7[a]	2.97 ± 0.10	1.12 ± 0.02	2.06 ± 0.08	0.93 ± 0.02	3.83	0.94	1.10	1.12	7.7×10^7
	37	23[b]	2.97 ± 0.01	1.22 ± 0.06	2.13 ± 0.02	0.95 ± 0.02	3.86	0.97	1.30	1.15	8.8×10^7
fcp1-1	24	6[c]	2.87 ± 0.02	0.92 ± 0.03	2.07 ± 0.02	0.93 ± 0.03	3.79	0.81	1.14	1.14	6.3×10^6
	37	4	3.07	1.55	2.18	0.94	3.79	0.96	1.09	1.11	3.2×10^6
	37	7[c]	2.97 ± 0.09	1.75 ± 0.04[d]	2.17 ± 0.04	0.96 ± 0.03	3.76	1.03	1.10	1.13	9.7×10^6
	37	23[b]	2.94 ± 0.02	2.12 ± 0.02[e]	2.12 ± 0.02	0.88 ± 0.00	3.90	1.24	1.08	1.10	8.4×10^5
thg1-Y146H	24	6[c]	2.95 ± 0.11	0.98 ± 0.06	1.89 ± 0.02	0.94 ± 0.04	3.82	0.82	1.18	1.11	1.4×10^7
	37	4	3.03	1.96	1.79	0.97	3.82	0.94	1.17	1.13	1.9×10^7
	37	7[c]	3.11 ± 0.04	2.40 ± 0.12[f]	1.95 ± 0.08	1.02 ± 0.01	3.78	1.01	1.13	1.14	2.3×10^7
	37	23	2.91	2.65	2.13	0.98	3.81	1.20	1.22	1.13	2.6×10^6
Expected mol/mol tRNA			3	1	2	1	4	1	1	1	

[a] $n = 4$, mean ± standard deviation.
[b] $n = 2$, mean ± standard deviation.
[c] $n = 3$, mean ± standard deviation.
[d] $tRNA^{His}$ m^5C, *fcp1-1* 24°C vs. 37°C 7 h: Student's *t*-test, $P = 5.4 \times 10^{-6}$.
[e] $tRNA^{His}$ m^5C, *fcp1-1* 24°C vs. 37°C 23 h: Student's *t*-test, $P = 7.0 \times 10^{-6}$.
[f] $tRNA^{His}$ m^5C, *thg1-Y146H* 24°C vs. 37°C 7 h: Student's *t*-test, $P = 2.1 \times 10^{-4}$.
[g] Viable cells per mL from a representative experiment.

examined modification status of tRNA^{His} in the BY4741 strain after growth into stationary phase and after nutrient starvation.

As BY4741 is grown in SD complete medium, we find that tRNA^{His} m^{5}C levels increase from 0.92 mol/mol tRNA in mid-log phase growth to 1.55 mol/mol tRNA in the first day of stationary phase and then gradually increase to 1.81 mol/mol tRNA over the next 5 d of stationary phase (Fig. 3, black bars). In contrast, during this time course, the control modifications (Am, Gm+ m^{1}G, D, and ψ) remain virtually unchanged in the tRNA^{His} (Fig. 3, light and dark gray bars; data not shown). The increase in m^{5}C seems to correlate with the diauxic shift, which transitions energy production from fermentation to respiration when glucose levels are low (Herman 2002). Accumulation of m^{5}C is not likely due to cell death since cells in stationary phase are known to be viable (Werner-Washburne et al. 1996; Allen et al. 2006).

We also find that levels of tRNA^{His} m^{5}C increase following several nutrient starvation treatments of the BY4741 strain, in each case with no significant loss of cell viability (Table 3). We find that m^{5}C levels increase significantly following 6 h of starvation for histidine (from 0.86 to 1.80 mol/mol tRNA) and following 24 h of starvation for histidine (to 2.00 mol/mol tRNA), for leucine (to 1.66 mol/mol tRNA), and for a combination of amino acids and uracil (SD minimal; to 1.68 mol/mol tRNA). m^{5}C levels also significantly increase to 1.53 mol/mol tRNA following 24 h of growth in SD complete medium, because the cells had reached saturation. In contrast, we observe a more modest increase in m^{5}C levels following 24 h of starvation for glucose (to 1.32 mol/mol tRNA), and a minimal increase following 24 h of starvation for uracil (to 1.23 mol/mol tRNA). The BY4741 strain viable cell titer remained constant during all of these treatments (Table 3), although cell growth ceased by ~3 h in each case (data not shown).

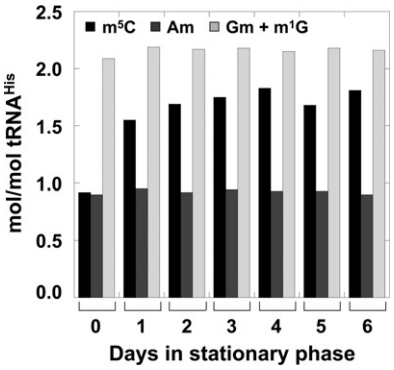

FIGURE 3. tRNA^{His} m^{5}C levels increase when BY4741 is grown to stationary phase. tRNA^{His} was purified from BY4741 grown in SD complete media in mid-log phase and in stationary phase for the indicated number of days. Nucleoside modifications were analyzed by HPLC, and m^{5}C (black), Am (dark gray), and m^{1}G + Gm (light gray) values are plotted over time. Other control modifications (dihydrouridine and pseudouridine) were unchanged during the time course (data not shown). The increase in m^{5}C levels between log phase growth and Day 1 of stationary phase is highly reproducible (Day 0 log phase, m^{5}C = 0.86 ± 0.03, n = 6; Day 1 stationary phase, m^{5}C = 1.53 ± 0.11, n = 7, mean ± standard deviation) (see Table 3).

It is likely that Trm4 is responsible for the additional m^{5}C modifications observed in tRNA^{His} under these conditions, for two reasons. First, Trm4 is the only known *S. cerevisiae* m^{5}C methyltransferase and can catalyze m^{5}C formation on substrate tRNAs at C_{34}, C_{40}, C_{48}, and C_{49} (Motorin and Grosjean 1999). Second, *trm4*-Δ mutants depleted of Thg1 lack all m^{5}C, including the additional m^{5}C found in tRNA^{His} at C_{48} and C_{50} (Gu et al. 2005). Consistent with this, we find that deletion of *TRM4* abolishes the accumulation of m^{5}C in tRNA^{His} that occurs upon histidine starvation of BY4741 (Table 3), suggesting that Trm4 catalyzes formation of the additional m^{5}C on tRNA^{His} during starvation conditions.

The *GCN4* pathway is not responsible for additional m^{5}C levels on tRNA^{His}

Since we observed significant increases in m^{5}C on tRNA^{His} after starving BY4741 for amino acids and only a marginal increase following starvation for uracil, we reasoned that additional m^{5}C might result from activation of the general amino acid starvation pathway. Indeed, we had previously shown that depletion of Thg1 leads to activation of the *GCN4* pathway, in addition to the accumulation of m^{5}C on tRNA^{His} (Gu et al. 2005). Thus, as expected, our amino acid starvation conditions lead to increased levels of both *HIS5* and *LYS1* mRNAs (Table 3; data not shown), which are known to be under *GCN4* control (Natarajan et al. 2001).

Two lines of evidence suggest that the increased m^{5}C levels observed in tRNA^{His} during starvation are not due to the *GCN4* pathway. First, we find nearly identical levels of elevated m^{5}C in tRNA^{His} after 5 h of histidine starvation of wild-type (0.86 to 1.71 mol/mol tRNA) and *gcn4*-Δ strains (0.83 to 1.65 mol/mol tRNA) (Table 4), while control modifications (D, ψ, Gm, m^{1}G, and Am) are virtually unchanged (Table 4; data not shown). Second, induction of the *GCN4* pathway by overexpression of *GCN4* from the P_{GAL} promoter, using the yeast movable ORF (MORF) collection (Gelperin et al. 2005), does not affect m^{5}C levels of tRNA^{His} (Table 5). Accordingly, although overexpression of *GCN4*-MORF in galactose dramatically increases mRNA levels of the known Gcn4 targets *HIS5* and *LYS1* relative to levels observed in glucose-containing media, there is only a very limited effect on m^{5}C levels of tRNA^{His} (from 0.89 to 0.98 mol/mol tRNA). Similarly, there is no effect on m^{5}C levels of tRNA^{His} when the vector control strain is grown in galactose (from 0.87 to 0.89 mol/mol tRNA) or when a control MORF construct (*ERV25*-MORF) is expressed in galactose (from 0.86 to 0.97 mol/mol tRNA). However, we note that our growth conditions do allow for an increase in tRNA^{His} m^{5}C, since overexpression of *TRM4*-MORF increases tRNA^{His} m^{5}C levels to 1.59 mol/mol tRNA (Table 5). Thus, we conclude that tRNA^{His} m^{5}C levels are not the result of *GCN4* pathway induction.

TABLE 3. $tRNA^{His}$ m^5C levels increase following starvation for amino acids or glucose

		BY4741						*trm4*-Δ	W303/CRY1	*TRM4*-cMORF
Media	Time (h)	ψ	m^5C	Gm + m^1G	Am	Viable cells/mL[p]	*HIS5*/*ACT1* [q]	m^5C	m^5C	m^5C
SD complete	0[a,b]	2.82 ± 0.04	0.86 ± 0.03	2.05 ± 0.02	0.87 ± 0.02	1.5×10^6	1.0	0.02	0.73	0.96
	6[c]	2.86 ± 0.06	0.93 ± 0.11	2.08 ± 0.05	0.90 ± 0.04	1.8×10^7	0.3	0.02	0.73	0.85
	24[d]	2.91 ± 0.06	1.53 ± 0.11[g]	2.15 ± 0.02	0.91 ± 0.04	3.8×10^7	ND	0.01	1.47	1.38
SD minimal	0[a]	2.82 ± 0.04	0.86 ± 0.03	2.05 ± 0.02	0.87 ± 0.02	5.8×10^6	ND	ND	ND	ND
	6[e]	2.92 ± 0.09	1.31 ± 0.12[h]	2.11 ± 0.09	0.90 ± 0.06	5.5×10^6	27.1	ND	ND	ND
	24[e]	2.95 ± 0.07	1.68 ± 0.05[i]	2.14 ± 0.05	0.92 ± 0.03	4.2×10^6	ND	ND	ND	ND
SD – His	0[a]	2.82 ± 0.04	0.86 ± 0.03	2.05 ± 0.02	0.87 ± 0.02	6.0×10^6	ND	0.02	0.73	0.96
	6[b]	2.97 ± 0.07	1.80 ± 0.08[j]	2.12 ± 0.01	0.94 ± 0.03	6.6×10^6	55.9	0.03	1.83	1.71
	24[d]	2.96 ± 0.06	2.00 ± 0.13[k]	2.13 ± 0.04	0.92 ± 0.03	4.9×10^6	ND	0.02	1.94	1.94
SD – Leu	0[a]	2.82 ± 0.04	0.86 ± 0.03	2.05 ± 0.02	0.87 ± 0.02	5.6×10^6	ND	ND	ND	0.96
	6[e]	2.94 ± 0.07	1.33 ± 0.07[l]	2.16 ± 0.02	0.92 ± 0.03	5.9×10^6	22.2	ND	ND	1.30
	24[e]	2.92 ± 0.10	1.66 ± 0.04[m]	2.19 ± 0.00	0.91 ± 0.03	4.5×10^6	ND	ND	ND	1.57
SD – Ura	0[a]	2.82 ± 0.04	0.86 ± 0.03	2.05 ± 0.02	0.87 ± 0.02	5.7×10^6	ND	ND	ND	ND
	6[f]	2.91 ± 0.10	1.16 ± 0.09[n]	2.15 ± 0.02	0.92 ± 0.04	4.9×10^6	0.9	ND	ND	ND
	24[f]	2.89 ± 0.08	1.23 ± 0.08[o]	2.17 ± 0.02	0.92 ± 0.03	5.5×10^6	ND	ND	ND	ND
S complete no glucose	0[a]	2.82 ± 0.04	0.86 ± 0.03	2.05 ± 0.02	0.87 ± 0.02	5.7×10^6	ND	ND	ND	ND
	6	2.87	1.16	2.17	0.90	6.1×10^6	ND	ND	ND	ND
	24	2.85	1.32	2.14	0.89	5.6×10^6	ND	ND	ND	ND
Expected mol/mol tRNA		3	1	2	1			1	1	1

(ND) Not determined.
[a]For each strain, one starting culture was split into the indicated media. Thus, each media condition has the same modification values at 0 h.
[b]$n = 6$, mean ± standard deviation.
[c]$n = 5$, mean ± standard deviation.
[d]$n = 7$, mean ± standard deviation.
[e]$n = 4$, mean ± standard deviation.
[f]$n = 3$, mean ± standard deviation.
[g–o]Student's *t*-test *P* values compare $tRNA^{His}$ m^5C levels between each growth condition and SD complete 0h. SD complete 24 h: [g]$P = 8.0 \times 10^{-7}$; SD minimal 6 h: [h]$P = 2.3 \times 10^{-3}$; 24 h: [i]$P = 5.0 \times 10^{-6}$; SD – His 6 h: [j]$P = 6.6 \times 10^{-8}$; 24 h: [k]$P = 7.6 \times 10^{-8}$; SD – Leu 6 h: [l]$P = 2.3 \times 10^{-4}$; 24 h: [m]$P = 1.1 \times 10^{-7}$; SD – Ura 6 h: [n]$P = 1.4 \times 10^{-2}$; 24 h: [o]$P = 6.1 \times 10^{-3}$.
[p]Viable cells per mL from a representative experiment.
[q]Normalized to *HIS5/ACT1* values of SD complete 0 h.

$tRNA^{His}$ m^5C levels increase during prolonged inhibition of the target of rapamycin pathway

We also tested the role of the TOR pathway in the induction of additional m^5C. The TOR pathway is another mechanism by which yeast respond to nutrient deprivation. In yeast, Tor1 and Tor2 can form two distinct multiprotein complexes: TORC1 (containing either Tor1 or Tor2), which is inhibited by rapamycin; and TORC2 (containing Tor2), which is insensitive to rapamycin (Loewith et al. 2002). To inhibit TORC1, we sought to treat cells with rapamycin, but BY4741 is relatively insensitive to rapamycin treatment when *TOR1* is present (data not shown). Therefore, we used the W303/CRY1 strain, after first showing that BY4741 and W303/CRY1 had virtually

TABLE 4. $tRNA^{His}$ m^5C levels during inhibition of starvation pathways

Strain	Media	Time (h)	ψ	m^5C	$Gm + m^1G$	Viable cells/mL[e]
BY4741	SD complete	0[a,b]	2.83 ± 0.05	0.86 ± 0.03	2.04 ± 0.03	2.5×10^6
		3	ND	ND	ND	8.8×10^6
		5[b]	2.85 ± 0.02	0.90 ± 0.04	2.04 ± 0.04	2.3×10^7
	SD – His	0[a,b]	2.83 ± 0.05	0.86 ± 0.03	2.04 ± 0.03	6.4×10^6
		3	ND	ND	ND	8.3×10^6
		5[b]	2.98 ± 0.04	1.71 ± 0.05[c]	2.05 ± 0.04	1.1×10^7
gcn4-Δ	SD complete	0[a,b]	2.84 ± 0.05	0.83 ± 0.05	2.06 ± 0.02	1.9×10^6
		3	ND	ND	ND	9.0×10^6
		5[b]	2.85 ± 0.06	0.83 ± 0.02	2.10 ± 0.05	2.2×10^7
	SD – His	0[a,b]	2.84 ± 0.05	0.83 ± 0.05	2.06 ± 0.02	5.0×10^6
		3	ND	ND	ND	6.8×10^6
		5[b]	2.91 ± 0.04	1.65 ± 0.10[d]	2.01 ± 0.06	8.7×10^7
W303/CRY1	YPD 0 nM Rapamycin	0	2.89	0.84	2.11	2.5×10^5
		4.5	3.03	1.02	2.15	3.0×10^6
	YPD 100 nM Rapamycin	0	2.89	0.84	2.11	2.0×10^6
		4.5	2.91	1.39	2.16	1.9×10^6
Expected mol/mol tRNA			3	1	2	

(ND) Not determined.
[a]For each strain, one starting culture was split into the indicated media. Thus, each media condition has the same modification values at 0 h.
[b]$n = 3$, mean ± standard deviation.
[c]$tRNA^{His}$ m^5C, BY4741 SD complete 0 h vs. SD – His 5 h: Student's *t*-test, $P = 2.8 \times 10^{-5}$.
[d]$tRNA^{His}$ m^5C, *gcn4-Δ* SD complete 0 h vs. SD – His 5 h: Student's *t*-test, $P = 5.6 \times 10^{-4}$.
[e]Viable cells per mL from a representative experiment.

identical increases in $tRNA^{His}$ m^5C levels after histidine starvation, while all other modifications (D, ψ, Gm, m^1G, and Am) were unaffected by starvation (Table 3; data not shown). Growth arrest triggered by rapamycin treatment (50, 100, and 150 nM) was apparent by 1.5–2 h, and we observed significant decreases in cell viability after treatment with 100 nM and 150 nM rapamycin for longer than 4.5 h (data not shown). However, we did observe increases in m^5C levels following several treatments with rapamycin that did not lead to loss of viability. We detected a modest increase in $tRNA^{His}$ m^5C levels when cells were treated with 150 nM rapamycin for 3 h (from 0.89 ± 0.01 to 1.18 ± 0.03 mol/mol tRNA, mean ± standard deviation; $n = 2$) (data not shown) and greater increases when cells were treated with 100 nM rapamycin for 4.5 h (from 0.84 to 1.39 mol/mol tRNA) (Table 4) or with 50 nM rapamycin for 24 h (from 0.84 to 1.73 mol/mol tRNA) (data not shown), without loss of viability. In each of these cases, we observe no change in all other $tRNA^{His}$ modifications (Table 4; data not shown). These data suggest that inhibition of the TOR pathway or the resulting G1 cell cycle arrest (Kunz et al. 1993; Barbet et al. 1996; Helliwell et al. 1998) can trigger additional m^5C levels on $tRNA^{His}$.

TABLE 5. Quantification of tRNA nucleoside modifications following *GCN4* and *TRM4* overexpression

BY4741 + MORF plasmid	S – Ura Media	*HIS5/ACT1*[a]	*LYS1/ACT1*[b]	$tRNA^{His}$ ψ	$tRNA^{His}$ m^5C	$tRNA^{His}$ $Gm + m^1G$	$tRNA^{His}$ Am	$tRNA^{Val(AAC)}$ ψ	$tRNA^{Val(AAC)}$ m^5C	$tRNA^{Val(AAC)}$ m^1G	$tRNA^{Gly(GCC)}$ ψ	$tRNA^{Gly(GCC)}$ m^5C	$tRNA^{Gly(GCC)}$ m^1G
P_{GAL} *GCN4*	Raff Gal	39.2[a]	51.7[a]	2.86	0.98	2.17	0.91	ND	ND	ND	ND	ND	ND
	Glucose	1.2[b]	1.3[b]	2.83	0.89	2.11	0.90	ND	ND	ND	ND	ND	ND
P_{GAL} *TRM4*	Raff Gal	ND	ND	2.84	1.59	2.12	0.92	4.13	1.53	1.13	3.88	1.98	1.05
	Glucose	ND	ND	2.85	0.86	2.08	0.88	4.04	0.80	1.00	3.90	1.56	1.04
P_{GAL} *ERV25*	Raff Gal	ND	ND	2.78	0.97	2.14	0.88	ND	ND	ND	ND	ND	ND
	Glucose	ND	ND	2.87	0.86	2.09	0.89	ND	ND	ND	ND	ND	ND
BG1766 (vector)	Raff Gal	1.0[a]	1.0[a]	2.83	0.89	2.12	0.88	3.70	0.87	1.10	3.96	1.69	1.08
	Glucose	1.0[b]	1.0[b]	2.80	0.87	2.07	0.87	4.18	0.96	1.08	3.81	1.54	1.02
Expected mol/mol tRNA				3	1	2	1	4	1	1	4	1	1

(ND) Not determined.
[a]Normalized to *HIS5/ACT1* or *LYS1/ACT1* values of BG1766 in S – Ura + Raffinose + Galactose media.
[b]Normalized to *HIS5/ACT1* or *LYS1/ACT1* values of BG1766 in S – Ura + Glucose media.

Trm4 protein levels do not increase during starvation conditions

A simple explanation for the increase in $tRNA^{His}$ m^5C levels is that Trm4 is more highly expressed during starvation conditions. To monitor endogenous Trm4 levels during starvation, we first inserted a chromosomal affinity tag derived from the MORF library (Gelperin et al. 2005) immediately 5′ of the *TRM4* stop codon to encode a Trm4-cMORF fusion. We then assayed $tRNA^{His}$ m^5C levels before and after amino acid starvation, demonstrating that the tag did not alter levels of m^5C in $tRNA^{His}$ compared to those in a wild-type strain (Table 3), and using cells from the same growth, we extracted cell lysate and measured Trm4 protein levels by Western blotting for the HA epitope. Control modifications (D, ψ, Gm, m^1G, and Am) remained constant over the time course of growth (data not shown). However, although $tRNA^{His}$ m^5C levels are elevated at 24 h in both the wild-type and the *TRM4*-cMORF strain (Table 3), we find that Trm4 protein levels appear to decrease at the 24-h time point (Fig. 4), consistent with experiments that demonstrate reductions in *TRM4* mRNA levels (Natarajan et al. 2001) and ribosome occupancy (Ingolia et al. 2009) following starvation.

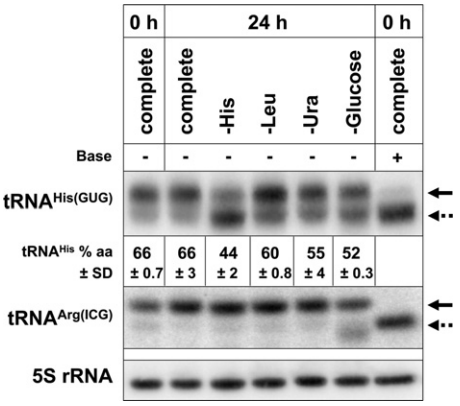

FIGURE 5. Analysis of $tRNA^{His}$ aminoacylation under different starvation conditions. RNA from the wild-type (BY4741) strain grown in the indicated media was isolated in acidic conditions to preserve aminoacylation, and 2 µg of RNA were resolved on an acidic gel, analyzed by Northern blot for $tRNA^{His}$, $tRNA^{Arg(ICG)}$, and 5S rRNA, and quantified using ImageQuant software. A control sample was treated with base (+) to detect migration of deacylated tRNA. (Solid arrows) Aminoacyl-tRNA, (dotted arrows) deacyl-tRNA. Each percent aminoacylation value is the mean ± standard deviation (SD) from two independent cultures. A representative Northern blot from one of the two independent cultures is shown.

Aminoacylation status of $tRNA^{His}$ is variably affected by different starvation conditions

Starvation for a particular amino acid in yeast and in *Escherichia coli* has been shown to affect the charging status of the corresponding tRNA isoacceptors, with some effects on other tRNAs (Dittmar et al. 2005; Zaborske et al. 2009). Therefore, $tRNA^{His}$ aminoacylation status may be affected by the starvation conditions that we examined, and changes in $tRNA^{His}$ aminoacylation levels might correlate with the amount of additional m^5C added to $tRNA^{His}$. To address this possibility, we starved the BY4741 strain for histidine, leucine, uracil, or glucose, or grew BY4741 to stationary phase and extracted RNA in acidic conditions to preserve tRNA aminoacylation. We performed the experiment with two independent cultures which serve as biological replicates. A Northern blot of samples from one of the replicates is shown in Figure 5. Prior to starvation, when the cultures are growing in log phase (SD complete 0 h), $tRNA^{His}$ is 66% aminoacylated. Following 24 h of starvation for histidine, leucine, uracil, or glucose, $tRNA^{His}$ is 44%, 60%, 55%, and 52% aminoacylated, respectively. Furthermore, following 24 h of growth in SD complete medium (stationary phase), $tRNA^{His}$ is 66% aminoacylated. These data suggest that aminoacylation levels do not directly correlate with additional m^5C levels. Although histidine starvation induces the most additional m^5C and the $tRNA^{His}$ is the most deacylated, we observe no change in aminoacylation levels of $tRNA^{His}$ following entry into stationary phase (Fig. 5), although $tRNA^{His}$ m^5C levels increase by 0.67 mol/mol tRNA (Table 3). In addition, $tRNA^{His}$ is more aminoacylated following leucine starvation than following uracil or glucose starvation (Fig. 5), but leucine starvation induces more additional m^5C than uracil or glucose (Table 3).

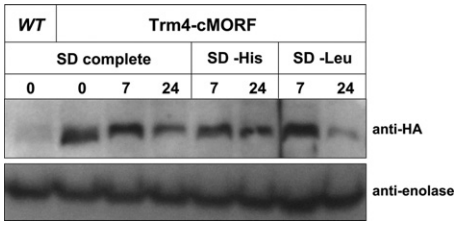

FIGURE 4. Trm4-cMORF levels do not increase during starvation. BY4741 and Trm4-cMORF strains were grown in SD complete, SD – His, or SD – Leu media and grown for 24 h at 30°C. Crude extracts were prepared at 0, 7, and 24 h, and 30 µg of protein were loaded in each lane and resolved by SDS-PAGE, followed by Western blotting. Anti-HA antibody was used to detect the cMORF tag on Trm4. BY4741 crude extract was used as a negative control. The same blot was incubated with anti-enolase antibody as a loading control.

Increases in m^5C levels are unique to $tRNA^{His}$

Since additional m^5C on $tRNA^{His}$ occurs at C_{48} and C_{50} (adjacent to m^5C_{49}) in Thg1-depleted cells (Gu et al. 2005), we examined $tRNA^{Gly(GCC)}$ and $tRNA^{Val(AAC)}$, two of the four additional tRNAs known to have m^5C_{49} and unmodified C_{48} and C_{50} (Juhling et al. 2009). Consistent with results from Thg1-depleted cells, we find little change in m^5C levels of these two tRNA species after starvation of wild-type cells (Table 6). Whereas histidine starvation for 24 h results in a large increase in $tRNA^{His}$ m^5C levels (from 0.86 to 2.00

TABLE 6. tRNA^{His}, tRNA$^{Val(AAC)}$, and tRNA$^{Gly(GCC)}$ m^{5}C levels during starvation

		tRNA^{His} [a]	tRNA$^{Val(AAC)}$ [b]				tRNA$^{Gly(GCC)}$ [b]			
Media	Time (h)	m^{5}C	ψ	m^{5}C	I	m^{1}G	ψ	m^{5}C	Cm	m^{1}G
SD complete	0	0.86 ± 0.03	3.76	0.79	0.96	1.10	3.53	1.44	0.75	1.03
	24[c]	1.53 ± 0.11	3.86	0.96	1.00	1.12	3.77	1.69	0.80	1.07
SD – His	6	1.80 ± 0.08	3.86	0.87	0.98	1.14	3.73	1.73	0.74	1.06
	24	2.00 ± 0.13	3.78	1.03	1.01	1.13	3.61	1.74	0.75	1.08
SD – Leu	24	1.66 ± 0.04	3.87	0.98	0.99	1.14	3.72	1.70	0.74	1.08
SD – Ura	24	1.23 ± 0.08	3.78	0.90	0.96	1.14	3.62	1.70	0.74	1.06
Expected mol/mol tRNA		1	4	1	1	1	4	1	1	1

[a]Values from Table 3.
[b]tRNA^{His}, tRNA$^{Val(AAC)}$, and tRNA$^{Gly(GCC)}$ were purified from bulk RNA extracted from the same growth.
[c]Stationary phase.

mol/mol tRNA), tRNA$^{Gly(GCC)}$ m^{5}C levels increase modestly (from 1.44 to 1.74 mol/mol tRNA), and tRNA$^{Val(AAC)}$ m^{5}C levels barely increase (from 0.79 to 1.03 mol/mol tRNA) (Fig. 6; Table 6). Similarly, leucine starvation for 24 h results in a substantial increase in tRNA^{His} m^{5}C levels (from 0.86 to 1.66 mol/mol tRNA) but only modest increases in m^{5}C levels of tRNA$^{Gly(GCC)}$ (from 1.44 to 1.70 mol/mol tRNA) and tRNA$^{Val(AAC)}$ (from 0.79 to 0.98 mol/mol tRNA). Control modification levels for each tRNA remain normal during these treatments (Table 6; data not shown). Furthermore, m^{5}C levels only slightly increase in tRNA$^{Val(AAC)}$ when temperature-sensitive strains are shifted to 37°C, relative to the drastic induction of additional m^{5}C in tRNA^{His} (Fig. 2B; Table 2). Thus, we infer that m^{5}C accumulation occurs preferentially on tRNA^{His} in conditions where cells stop growing.

In support of this claim, both tRNA$^{Val(AAC)}$ and tRNA$^{Gly(GCC)}$ have the capacity to acquire additional m^{5}C after overexpression of *TRM4*-MORF (Table 5). Strikingly, *TRM4* overexpression results in a nearly identical increase in m^{5}C levels of tRNA^{His} (from 0.86 to 1.59 mol/mol tRNA) and tRNA$^{Val(AAC)}$ (from 0.80 to 1.53 mol/mol tRNA) and a smaller but still significant increase in m^{5}C levels of tRNA$^{Gly(GCC)}$ (from 1.56 to 1.98 mol/mol tRNA), whereas all other control modifications (D, ψ, Gm, m^{1}G, I, Cm, and Am) are normal (Table 5; data not shown). Since both tRNA$^{Val(AAC)}$ and tRNA$^{Gly(GCC)}$ can be modified with additional m^{5}C in vivo by Trm4 but are not substrates for additional m^{5}C modification (presumably by Trm4) during growth arrest conditions, we conclude that the additional m^{5}C during growth arrest is specific to tRNA^{His}.

DISCUSSION

We have demonstrated here that m^{5}C levels of tRNA^{His} are unusually responsive to a number of different conditions in which yeast cells stop growing. We had previously shown that tRNA^{His} accumulates additional m^{5}C at C_{48} and C_{50} in the variable loop, adjacent to m$^5C_{49}$, following depletion of Thg1 and the subsequent growth arrest (Gu et al. 2005). We have extended this analysis to show that tRNA^{His} has additional m^{5}C when either *thg1* temperature-sensitive strains or temperature-sensitive strains unrelated to tRNA function are grown at nonpermissive temperature and when wild-type strains such as BY4741 are grown to saturation or are starved for histidine, amino acids, leucine, or (to a lesser extent) for glucose or uracil. In the majority of these cases, the accumulation of additional m^{5}C on tRNA^{His} is not caused by loss of cell viability. In addition, we have shown that the accumulation of additional m^{5}C on tRNA^{His} is not due to induction of the *GCN4* pathway and is not due to an increase in Trm4 protein levels during our starvation conditions, although the additional m^{5}C modification is absent in a *trm4*-Δ mutant. Remarkably, this additional m^{5}C specifically occurs on tRNA^{His}, and not on two other possible substrates, tRNA$^{Val(AAC)}$ or tRNA$^{Gly(GCC)}$, that also have m$^5C_{49}$ flanked by cytidines, although these tRNA species can acquire more m^{5}C when Trm4 is overproduced.

The molecular signals that trigger Trm4 to modify tRNA^{His} with additional m^{5}C during growth arrest conditions remain

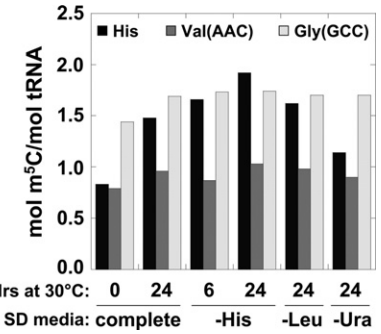

FIGURE 6. m^{5}C increases specifically on tRNA^{His} during starvation. tRNA^{His} (black), tRNA$^{Val(AAC)}$ (dark gray), and tRNA$^{Gly(GCC)}$ (light gray) were purified from BY4741 grown in the indicated starvation conditions. Nucleoside modifications were analyzed by HPLC, and m^{5}C values are plotted over time for each tRNA.

unclear. Although $tRNA^{His}$ localizes to the nucleus following Thg1 depletion (Gu et al. 2005), and Trm4 is a nuclear protein (Wu et al. 1998), our data suggest that modulation of tRNA subcellular dynamics is not the sole contributor to additional m^5C levels, since glucose starvation results in rapid accumulation of tRNAs in the nucleus (Shaheen and Hopper 2005; Whitney et al. 2007), but we observe only modest accumulation of m^5C relative to that observed with histidine or leucine starvation. Three lines of evidence suggest that tRNA charging status is also not the sole contributor to additional m^5C on $tRNA^{His}$. First, $tRNA^{His}$ from a *thg1*-Δ strain has normal m^5C levels, despite the fact that the tRNA is mostly deacylated (Preston and Phizicky 2010). Second, $tRNA^{His}$ has an additional 0.80 mol m^5C/mol tRNA (Table 3) following 24 h of leucine starvation, although $tRNA^{His}$ aminoacylation status is virtually unaffected (Fig. 5). Third, $tRNA^{His}$ m^5C increases by 0.67 mol/mol tRNA (Table 3) when wild-type cells are grown to stationary phase and $tRNA^{His}$ aminoacylation levels are unaltered (Fig. 5).

However, it remains possible that both deacylation of $tRNA^{His}$ and its presence in the nucleus contribute to the additional m^5C that we observe. This would be consistent with the observation that more m^5C accumulates on $tRNA^{His}$ during histidine starvation than during other starvation conditions. Furthermore, increased m^5C on $tRNA^{His}$ occurs when tRNAs are known to accumulate in the nucleus: during starvation for amino acids, starvation for glucose, and as cells enter late-log and near-stationary phase (Whitney et al. 2007). Indeed, we previously showed that the additional m^5C that accumulates upon Thg1 depletion occurs at a time when $tRNA^{His}$ is deacylated and is localized to the nucleus (Gu et al. 2005), and it is known that both charged and uncharged tRNA can accumulate in the nucleus during starvation (Whitney et al. 2007). It is not completely clear why different levels of $tRNA^{His}$ m^5C arise during leucine starvation compared to glucose starvation; however, it is clear that different stress conditions have different effects on the cell since they elicit transcriptionally distinct types of growth arrest (Gasch et al. 2000; Boer et al. 2008; Brauer et al. 2008; Klosinska et al. 2011).

The specificity of additional m^5C modification for $tRNA^{His}$ is also puzzling. Although overproduction of Trm4 results in similar levels of additional m^5C on $tRNA^{His}$, $tRNA^{Val(AAC)}$, and $tRNA^{Gly(GGC)}$, the additional m^5C is much more specific for $tRNA^{His}$ after temperature shift of *fcp1*^{ts} or *thg1*^{ts} strains, after starvation of a wild-type strain for histidine or leucine, and after growth to stationary phase. Therefore, we presume that, under these conditions, $tRNA^{His}$ somehow becomes more accessible to Trm4, or Trm4 activity is altered, but it is not yet clear how this is accomplished. This specificity for $tRNA^{His}$ might possibly be explained by a unique structural property of $tRNA^{His}$ or by a secondary protein that binds $tRNA^{His}$ during growth arrest. One possibility is that specificity is related to the unique sensitivity of histidyl-$tRNA^{His}$ to deacylation in vitro (Chernyakov et al. 2008a; Preston and Phizicky 2010), and the observation that $tRNA^{His}$ is partially deacylated when isolated (Gu et al. 2005; Preston and Phizicky 2010), which could mean that this tRNA species is a cellular sensor for poor growth conditions.

Although our data demonstrate that the additional m^5C levels of $tRNA^{His}$ during histidine starvation accumulate independently of the *GCN4* gene and are not provoked by induction of the *GCN4* pathway, it is not clear if the accumulation of m^5C of $tRNA^{His}$ involves the TOR pathway, which also plays a role in stationary phase and quiescence (Herman 2002). We observe a distinct increase in $tRNA^{His}$ m^5C levels when cells are treated with rapamycin, but this increase is modest compared to other treatments. However, because rapamycin treatment results in G1 phase cell cycle arrest (Kunz et al. 1993; Barbet et al. 1996; Helliwell et al. 1998), it is difficult to determine whether the increased m^5C is due to inhibition of the TOR pathway or to the resulting growth arrest. It is intriguing to speculate that the TOR pathway is connected to the accumulation of m^5C in $tRNA^{His}$, because high-throughput studies have reported that deletion of *TRM4* results in increased rapamycin sensitivity (Parsons et al. 2004) and that overexpression of *TRM4* confers rapamycin resistance (Butcher et al. 2006), although we have not been able to observe such effects (data not shown).

The function of the additional m^5C of $tRNA^{His}$ has not yet been elucidated. Since overexpression of *TRM4*-MORF appears to increase m^5C levels of several tRNA species and causes a slow-growth phenotype (Yoshikawa et al. 2011; data not shown; JM Dewe and EM Phizicky, unpubl.), we infer that excess m^5C modification has a deleterious effect on function of one or more tRNAs. Conversely, m^5C modification of tRNAs can play a protective role during stress conditions. Amino acid starvation in *Tetrahymena* and oxidative stress in yeast, humans, and plants results in cleavage of tRNAs in the anti-codon loop (Lee and Collins 2005; Thompson et al. 2008), and the *Drosophila* m^5C methyltransferase Dnmt2 is important for viability during oxidative stress and heat shock conditions (Schaefer et al. 2010), because its modification of C_{38} in the anti-codon loop protects substrate tRNAs from cleavage by angiogenin in both *Drosophila* and mice (Goll et al. 2006; Schaefer et al. 2010). Thus, the additional m^5C of $tRNA^{His}$ may have a protective function, similar to the role of m^5C_{49} of $tRNA^{Val(AAC)}$ in reducing the extent of rapid decay of tRNAs lacking m^7G_{46} (Alexandrov et al. 2006; Chernyakov et al. 2008b; Dewe et al. 2012). Intriguingly, while preparing this manuscript, it was reported that hydrogen peroxide treatment leads to alteration of m^5C levels in yeast $tRNA^{Leu(CAA)}$, with 70% more m^5C_{34} and 20% less m^5C_{48}, and these changes were associated with increased expression of a ribosomal protein enriched with TTG codons (Chan et al. 2012). Further experiments will be required to fully understand the biology of m^5C, the cause of the additional m^5C of $tRNA^{His}$, and the role of the additional m^5C during growth arrest.

MATERIALS AND METHODS

Strain construction

Strains used in this study are listed in Table 7.

To construct the *gcn4*-Δ::*ble*^{R} (MBY934) strain, we amplified the phleomycin resistance cassette from the pUG66 plasmid (Gueldener et al. 2002) with GCN4 Up 179 + Phleo Forward (5′-ATCATGTA CCCGTAGAATTTTATTCAAGATGTTTCCGTAACGGCAGCTG AAGCTTCGTAC-3′) and GCN4 Down 312 + Phleo Reverse (5′-G CATTAGCTATAACACGTTAATATGGTGGAGTCAGCTGAGAA GGCATAGGCCACTAGTGG-3′) to add 43-nt sequence upstream of and downstream from *GCN4* to the Phleo cassette 5′ and 3′ ends, respectively. We extended the *GCN4* homologous regions to 87 nt by amplifying the first PCR product with GCN4 Up 223 (87) Forward (5′-ACTGTCAGTTTTTTGAAGAGTTATTTG TTTTGTTACCAATTGCTATCATGTACCCGTAGA-3′) and GC N4 Down 356 (87) Reverse (5′-CATGAGTACTCCTAAATAGGG CGATATTTTAAAGTTTCATTCCAGCATTAGCTATAACAC-3′). This extended PCR product was transformed into BY4741 as previously described (Sherman 1991) and selected on YPD media containing 8 µg/mL phleomycin (Chernyakov et al. 2008b). The *gcn4*-Δ::*ble*^{R} strain was verified by PCR.

The *TRM4*-cMORF strain, MBY1026B, was constructed in a manner similar to the *gcn4*-Δ::*ble*^{R} strain. We used the plasmid, AVA0258, which encodes the cMORF tag (consisting of His6, HA epitope, 3C protease site, ZZ protein A), followed by *Kluyveromyces lactis URA3* as a marker for insertion into the chromosome. We PCR-amplified this construct using TRM4 C-ter + TAP 5′ (5′-GAACCTCTA CTGAAGCTCCTAGCGCTGCTAATAACCCAGCTTTCTTGTA CAAAGTGG-3′; contains 43 nt corresponding to the C terminus of Trm4 without the stop codon and a 5′ portion of the cMORF tag sequence), and TRM4 Downstream (w/stop) + TAP 3′ (5′-CTTT ACAGTGGAGGGGATAAGAAACATGATAACTATCATACGACT CACTATAGGG-3′; inserts the Trm4 stop codon after the cMORF tag and *URA3* marker and contains 43 nt of the region downstream from *TRM4*). We then used this PCR product to extend the regions homologous to *TRM4* by PCR amplification with TRM4 C-ter extended (TAP) 5′ (5′-GACTGAATCTCCCGCAGAAACTACTA CCGGAACCTCTACTGAAGCTC-3′) and TRM4 Downstream extended (TAP) 3′ (5′-AGTATTATATTCTTATTTTTGCCTTTTAA TAATATACATTTACTTTACAGTGGAGGGGAT-3′). The resulting strain was verified by PCR.

We constructed *thg1* temperature-sensitive (*thg1*^{ts}) strains, MBY294 (*thg1-Y8C*), MBY289 (*thg1-G172D,L233S*), and MBY303 (*thg1-Y146H*) in two steps. First, we randomly mutagenized a single copy *THG1* plasmid, screened for temperature sensitivity in a *thg1*-Δ strain, and sequenced the resulting alleles. We then inserted these *thg1*^{ts} alleles and wild-type *THG1* into the *THG1* locus by transformation of the SC1300-2 strain in which *THG1* was deleted with a *LEU2,CYH2* cassette in a *cyh*^{r} background, and selected for cycloheximide resistance, accompanied by leucine auxotrophy. Temperature sensitivity was confirmed and complemented by a wild-type copy of *THG1*.

Strain starvation

Strains were grown to log phase at 30°C in SD complete media, then spun down and resuspended in the following media conditions: SD complete, SD minimal (contains only yeast nitrogen base and glucose), SD − His, SD − Leu, SD − Ura, or S complete no glucose. These cultures were grown for 24 h at 30°C, and cells were harvested for analysis of tRNA modifications at indicated times.

Temperature-sensitive strain growth

Strains were grown to log phase in YPD at 24°C, diluted to OD_{600} = 0.5 and grown at either 24°C or 37°C for the time indicated.

Rapamycin treatment of W303/CRY1

W303 was pretreated with DMSO by growing in YPD media containing 1% DMSO overnight until the strain reached early log phase. Cells were harvested prior to drug treatment and after growth in the

TABLE 7. Strains used in this study

Strain	Genotype	Parent	Source
BY4741	*MAT* **a** *his3Δ1 leu2Δ0 met15Δ0 ura3Δ0*		Open Biosystems
W303/CRY1	*MAT* α *ade2-1 can1-100 his3-11 leu2-3,112 trp1-1 ura3-1*		D. Krysan
SC1300-2	*MAT* **a** *his3Δ1 leu2Δ0 met15Δ0 ura3Δ0 cyh*^{r} *thg1-Δ0::LEU2,CYH2* [*CEN URA3* P_{GAL} *THG1*]	BY4741	This study
MBY289	*MAT* **a** *his3Δ1 leu2Δ0 met15Δ0 ura3Δ0 cyh*^{r} *thg1-G172D/L233S*	SC1300-2	This study
MBY294	*MAT* **a** *his3Δ1 leu2Δ0 met15Δ0 ura3Δ0 cyh*^{r} *thg1-Y8C*	SC1300-2	This study
MBY303	*MAT* **a** *his3Δ1 leu2Δ0 met15Δ0 ura3Δ0 cyh*^{r} *thg1-Y146H*	SC1300-2	This study
MBY308	*MAT* **a** *his3Δ1 leu2Δ0 met15Δ0 ura3Δ0 cyh*^{r} *THG1*	SC1300-2	This study
MBY480	*MAT* **a** *thg1-Δ0:kanMX* [2µ *LEU2* tRNA^{His} A_{73}, 2µ *HIS3* P_{HTS1}-*HTS1*]	BY4741	(Preston and Phizicky 2010)
Y08328	*MAT* **a** *his3Δ1 leu2Δ0 met15Δ0 ura3Δ0 abf1-102*	BY4741	C. Boone
Y09266	*MAT* **a** *his3Δ1 leu2Δ0 met15Δ0 ura3Δ0 fcp1-1*	BY4741	C. Boone
	MAT **a** *his3Δ1 leu2Δ0 met15Δ0 ura3Δ0 cdc48-9(Y-F)*	BY4741	C. Boone
MBY934A,B	*MAT* **a** *his3Δ1 leu2Δ0 met15Δ0 ura3Δ0 gcn4-Δ::ble*^{R}	BY4741	This study
MBY1026B	*MAT* **a** *his3Δ1 leu2Δ0 met15Δ0 ura3Δ0 TRM4-cMORF(His$_6$-HA epitope-3C site-ZZ protein A)-K. lactis URA3*	BY4741	This study
MBY687A	*MAT* **a** *his3Δ1 leu2Δ0 met15Δ0 ura3Δ0 trm4-Δ::kanMX*	BY4741	This study

presence of the indicated concentration of rapamycin or 1% DMSO for the indicated amount of time.

Assessment of viable cell titer

For each condition, a given volume of culture was plated onto YPD plates. Cells were grown for 3 d at 30°C or at 24°C for temperature-sensitive strains, and colonies were counted and normalized to the volume plated to calculate viable cells per milliliter of culture.

Bulk RNA isolation and purification of tRNA

Bulk low molecular weight RNA was isolated from 150 to 300 OD of yeast cells that were grown in conditions described above, using a hot phenol extraction method, as described elsewhere (Kotelawala et al. 2008). Total RNA was extracted from stationary phase cells by lysis with glass beads, phenol-chloroform extraction, and ethanol precipitation, as described previously (Letzring et al. 2010). tRNAs were purified using 5′ biotinylated DNA oligomers complementary to the following: nt 48–72 for $tRNA^{His}$ (5′ Bio $tRNA^{His}$: 5′-/Biotin/GCCATCTCCTAGAATCGAACCAGGG-3′) (Preston and Phizicky 2010), nt 52–76 for $tRNA^{Gly(GCC)}$ (BioGly: 5′-/Biotin/TGGTGCG CAAGCCCGGAATCGAACC-3′) (Gu et al. 2005), and nt 55–76 for $tRNA^{Val(AAC)}$ (Biotin-tRNAVal1: 5′-/Biotin/TGGTGATTTCGCCC AGGATCGA-3′). For each tRNA purified, 22.5 pmol of oligomer were first bound to streptavidin magnetic particles (Roche). Then, bulk RNA (1–1.25 mg) was added to oligomer-bound beads in the presence of 2.4 M tetraethylammonium chloride (TEACl; Sigma), washed, and the tRNA was melted off the oligomer at 60°C to obtain pure tRNA. The resulting tRNA was desalted and concentrated using Amicon Ultra 4 10,000 MWCO columns (Millipore).

HPLC analysis of tRNA nucleosides

tRNAs (1.25 µg) were digested at 37°C for at least 2 h using 0.5 µg P1 nuclease (MP Biomedicals) in a buffer containing 20 mM NaOAc pH 5.2 and 0.2 mM $ZnCl_2$ and then treated with calf intestinal phosphatase (Roche) for at least 1 h. Nucleosides were resolved by reverse-phase HPLC essentially as described (Gehrke and Kuo 1989), and each nucleoside was identified and quantified as described previously (Jackman et al. 2003; Kotelawala et al. 2008).

Quantitative RT-PCR

RNA was extracted using the hot phenol extraction method (Kotelawala et al. 2008) and treated with RQ1 RNase-free DNase (Promega), followed by a phenol-chloroform extraction, two chloroform extractions, and ethanol precipitation. This RNA was reverse transcribed with Superscript II Reverse Transcriptase (Invitrogen) using Random Primers (Invitrogen). Next, this DNA was PCR-amplified using Fast SYBR Green master mix (Applied Biosystems) and 0.2 µM each of 5′ and 3′ primers specific to *ACT1* (ACT1 Set 1 Forward 5′-ACGTTCCAGCCTTCTACGTTTCCA-3′ and ACT1 Set 1 Reverse 5′-ACGTGAGTAACACCATCACCGGAA-3′, *HIS5* (HIS5 Set 1 Forward 5′-AATGCCCATGGACCTACTCCAGTT-3′ and HIS5 Set 1 Reverse 5′-ACACCTAGGCACAGATTGTCAGCA -3′), or *LYS1* (LYS1 Set 1 Forward 5′-AGCAGACACTACCAA CCCTCACAA-3′ AND LYS1 Set 1 Reverse 5′-CTTGGCAGCAAA GAAGGCAAGTGA-3′), with the following amplification scheme: 95°C for 20 sec and then 40 cycles of 95°C for 3 sec and 60°C for 30 sec.

Analysis of aminoacylated RNA

RNA was isolated from 50 OD of cells in acidic conditions (pH 4.5), and 2 µg of RNA were resolved by PAGE under acidic conditions, as previously described (Chernyakov et al. 2008a), and transferred to Hybond N+ membrane (Amersham Biosciences). The membrane was UV cross-linked, hybridized with 5′-labeled oligomers tRNAHis (40–64) (5′-CTAGAATCGAACCAGGGTTTCATC-3′), ArgP1 (5′-TAGCCAGACGCCGTGAC-3′), and 5S RNA (5′-GGT AGATATGGCCGCAACC-3′) to detect $tRNA^{His}$, $tRNA^{Arg\ (ICG)}$, and 5S rRNA, and visualized with a Typhoon PhosphorImager (GE Healthcare).

ACKNOWLEDGMENTS

We thank Elizabeth Grayhack for invaluable insight and discussions throughout this work. We also thank Charlie Boone (U. Toronto) for the gift of temperature-sensitive yeast strains and Mark Dumont (U. Rochester) for the gift of enolase antibody. We thank Jason Salter and Jane Jackman for constructing the SC1300-2 strain used to generate the *thg1*^{ts} strains and Marv Wickens (U. Wisconsin–Madison) for the use of laboratory equipment to complete the experiment in Figure 5. This research is supported by NIH Grant GM52347 to E.M.P. M.A.P. was supported by NIH Training Grant in Cellular, Biochemical and Molecular Sciences 5T32 GM068411.

Received August 1, 2012; accepted October 24, 2012.

REFERENCES

Agris PF, Koh H, Soll D. 1973. The effect of growth temperatures on the in vivo ribose methylation of *Bacillus stearothermophilus* transfer RNA. *Arch Biochem Biophys* **154:** 277–282.

Agris PF, Vendeix FA, Graham WD. 2007. tRNA's wobble decoding of the genome: 40 years of modification. *J Mol Biol* **366:** 1–13.

Alexandrov A, Chernyakov I, Gu W, Hiley SL, Hughes TR, Grayhack EJ, Phizicky EM. 2006. Rapid tRNA decay can result from lack of nonessential modifications. *Mol Cell* **21:** 87–96.

Allen C, Buttner S, Aragon AD, Thomas JA, Meirelles O, Jaetao JE, Benn D, Ruby SW, Veenhuis M, Madeo F, et al 2006. Isolation of quiescent and nonquiescent cells from yeast stationary-phase cultures. *J Cell Biol* **174:** 89–100.

Barbet NC, Schneider U, Helliwell SB, Stansfield I, Tuite MF, Hall MN. 1996. TOR controls translation initiation and early G1 progression in yeast. *Mol Biol Cell* **7:** 25–42.

Bjork GR, Jacobsson K, Nilsson K, Johansson MJ, Bystrom AS, Persson OP. 2001. A primordial tRNA modification required for the evolution of life? *EMBO J* **20:** 231–239.

Boer VM, Amini S, Botstein D. 2008. Influence of genotype and nutrition on survival and metabolism of starving yeast. *Proc Natl Acad Sci* **105:** 6930–6935.

Brauer MJ, Huttenhower C, Airoldi EM, Rosenstein R, Matese JC, Gresham D, Boer VM, Troyanskaya OG, Botstein D. 2008. Coordination of growth rate, cell cycle, stress response, and metabolic activity in yeast. *Mol Biol Cell* **19:** 352–367.

Buchman AR, Kimmerly WJ, Rine J, Kornberg RD. 1988. Two DNA-binding factors recognize specific sequences at silencers, upstream

activating sequences, autonomously replicating sequences, and telomeres in *Saccharomyces cerevisiae*. *Mol Cell Biol* **8:** 210–225.

Butcher RA, Bhullar BS, Perlstein EO, Marsischky G, LaBaer J, Schreiber SL. 2006. Microarray-based method for monitoring yeast overexpression strains reveals small-molecule targets in TOR pathway. *Nat Chem Biol* **2:** 103–109.

Chan CT, Dyavaiah M, DeMott MS, Taghizadeh K, Dedon PC, Begley TJ. 2010. A quantitative systems approach reveals dynamic control of tRNA modifications during cellular stress. *PLoS Genet* **6:** e1001247. doi: 10.1371/journal.pgen.1001247.

Chan CT, Pang YL, Deng W, Babu IR, Dyavaiah M, Begley TJ, Dedon PC. 2012. Reprogramming of tRNA modifications controls the oxidative stress response by codon-biased translation of proteins. *Nat Commun* **3:** 937. doi: 10.1038/ncomms1938.

Chernyakov I, Baker MA, Grayhack EJ, Phizicky EM. 2008a. Identification and analysis of tRNAs that are degraded in *Saccharomyces cerevisiae* due to lack of modifications. *Methods Enzymol* **449:** 221–237.

Chernyakov I, Whipple JM, Kotelawala L, Grayhack EJ, Phizicky EM. 2008b. Degradation of several hypomodified mature tRNA species in *Saccharomyces cerevisiae* is mediated by Met22 and the 5′-3′ exonucleases Rat1 and Xrn1. *Genes Dev* **22:** 1369–1380.

Dewe JM, Whipple JM, Chernyakov I, Jaramillo LN, Phizicky EM. 2012. The yeast rapid tRNA decay pathway competes with elongation factor 1A for substrate tRNAs and acts on tRNAs lacking one or more of several modifications. *RNA* **18:** 1886–1896.

Dittmar KA, Sorensen MA, Elf J, Ehrenberg M, Pan T. 2005. Selective charging of tRNA isoacceptors induced by amino-acid starvation. *EMBO Rep* **6:** 151–157.

El Yacoubi B, Lyons B, Cruz Y, Reddy R, Nordin B, Agnelli F, Williamson JR, Schimmel P, Swairjo MA, de Crecy-Lagard V. 2009. The universal YrdC/Sua5 family is required for the formation of threonylcarbamoyladenosine in tRNA. *Nucleic Acids Res* **37:** 2894–2909.

Gasch AP, Spellman PT, Kao CM, Carmel-Harel O, Eisen MB, Storz G, Botstein D, Brown PO. 2000. Genomic expression programs in the response of yeast cells to environmental changes. *Mol Biol Cell* **11:** 4241–4257.

Gehrke CW, Kuo KC. 1989. Ribonucleoside analysis by reversed-phase high-performance liquid chromatography. *J Chromatogr* **471:** 3–36.

Gelperin DM, White MA, Wilkinson ML, Kon Y, Kung LA, Wise KJ, Lopez-Hoyo N, Jiang L, Piccirillo S, Yu H, et al 2005. Biochemical and genetic analysis of the yeast proteome with a movable ORF collection. *Genes Dev* **19:** 2816–2826.

Goll MG, Kirpekar F, Maggert KA, Yoder JA, Hsieh CL, Zhang X, Golic KG, Jacobsen SE, Bestor TH. 2006. Methylation of $tRNA^{Asp}$ by the DNA methyltransferase homolog Dnmt2. *Science* **311:** 395–398.

Grunberger D, Weinstein IB, Mushinski JF. 1975. Deficiency of the Y base in a hepatoma phenylalanine tRNA. *Nature* **253:** 66–67.

Grunberger D, Pergolizzi RG, Kuchino Y, Mushinski JF, Nishimura S. 1983. Alterations in post-transcriptional modification of the Y base in phenylalanine tRNA from tumor cells. *Recent Results Cancer Res* **84:** 133–145.

Gu W, Jackman JE, Lohan AJ, Gray MW, Phizicky EM. 2003. $tRNA^{His}$ maturation: An essential yeast protein catalyzes addition of a guanine nucleotide to the 5′ end of $tRNA^{His}$. *Genes Dev* **17:** 2889–2901.

Gu W, Hurto RL, Hopper AK, Grayhack EJ, Phizicky EM. 2005. Depletion of *Saccharomyces cerevisiae* $tRNA^{His}$ guanylyltransferase Thg1p leads to uncharged $tRNA^{His}$ with additional m^5C. *Mol Cell Biol* **25:** 8191–8201.

Gueldener U, Heinisch J, Koehler GJ, Voss D, Hegemann JH. 2002. A second set of loxP marker cassettes for Cre-mediated multiple gene knockouts in budding yeast. *Nucleic Acids Res* **30:** e23. doi: 10.1093/nar/30.6.e23.

Guy MP, Podyma BM, Preston MA, Shaheen HH, Krivos KL, Limbach PA, Hopper AK, Phizicky EM. 2012. Yeast Trm7 interacts with distinct proteins for critical modifications of the $tRNA^{Phe}$ anticodon loop. *RNA* **18:** 1921–1933.

Helliwell SB, Howald I, Barbet N, Hall MN. 1998. TOR2 is part of two related signaling pathways coordinating cell growth in *Saccharomyces cerevisiae*. *Genetics* **148:** 99–112.

Herman PK. 2002. Stationary phase in yeast. *Curr Opin Microbiol* **5:** 602–607.

Hosbach HA, Kubli E. 1979. Transfer RNA in aging *Drosophila*: II. Isoacceptor patterns. *Mech Ageing Dev* **10:** 141–149.

Ingolia NT, Ghaemmaghami S, Newman JR, Weissman JS. 2009. Genome-wide analysis in vivo of translation with nucleotide resolution using ribosome profiling. *Science* **324:** 218–223.

Ishida K, Kunibayashi T, Tomikawa C, Ochi A, Kanai T, Hirata A, Iwashita C, Hori H. 2011. Pseudouridine at position 55 in tRNA controls the contents of other modified nucleotides for low-temperature adaptation in the extreme-thermophilic eubacterium *Thermus thermophilus*. *Nucleic Acids Res* **39:** 2304–2318.

Jackman JE, Montange RK, Malik HS, Phizicky EM. 2003. Identification of the yeast gene encoding the tRNA m^1G methyltransferase responsible for modification at position 9. *RNA* **9:** 574–585.

Juhling F, Morl M, Hartmann RK, Sprinzl M, Stadler PF, Putz J. 2009. tRNAdb 2009: Compilation of tRNA sequences and tRNA genes. *Nucleic Acids Res* **37:** D159–D162.

Kadaba S, Krueger A, Trice T, Krecic AM, Hinnebusch AG, Anderson J. 2004. Nuclear surveillance and degradation of hypomodified initiator $tRNA^{Met}$ in *S. cerevisiae*. *Genes Dev* **18:** 1227–1240.

Kadaba S, Wang X, Anderson JT. 2006. Nuclear RNA surveillance in *Saccharomyces cerevisiae*: Trf4p-dependent polyadenylation of nascent hypomethylated tRNA and an aberrant form of 5S rRNA. *RNA* **12:** 508–521.

Kamenski P, Kolesnikova O, Jubenot V, Entelis N, Krasheninnikov IA, Martin RP, Tarassov I. 2007. Evidence for an adaptation mechanism of mitochondrial translation via tRNA import from the cytosol. *Mol Cell* **26:** 625–637.

Klosinska MM, Crutchfield CA, Bradley PH, Rabinowitz JD, Broach JR. 2011. Yeast cells can access distinct quiescent states. *Genes Dev* **25:** 336–349.

Kobor MS, Archambault J, Lester W, Holstege FC, Gileadi O, Jansma DB, Jennings EG, Kouyoumdjian F, Davidson AR, Young RA, et al 1999. An unusual eukaryotic protein phosphatase required for transcription by RNA polymerase II and CTD dephosphorylation in *S. cerevisiae*. *Mol Cell* **4:** 55–62.

Kotelawala L, Grayhack EJ, Phizicky EM. 2008. Identification of yeast tRNA Um44 2′-O-methyltransferase (Trm44) and demonstration of a Trm44 role in sustaining levels of specific $tRNA^{Ser}$ species. *RNA* **14:** 158–169.

Kuchino Y, Borek E. 1978. Tumour-specific phenylalanine tRNA contains two supernumerary methylated bases. *Nature* **271:** 126–129.

Kuchino Y, Shindo-Okada N, Ando N, Watanabe S, Nishimura S. 1981. Nucleotide sequences of two aspartic acid tRNAs from rat liver and rat ascites hepatoma. *J Biol Chem* **256:** 9059–9062.

Kuchino Y, Borek E, Grunberger D, Mushinski JF, Nishimura S. 1982. Changes of post-transcriptional modification of wye base in tumor-specific $tRNA^{Phe}$. *Nucleic Acids Res* **10:** 6421–6432.

Kunz J, Henriquez R, Schneider U, Deuter-Reinhard M, Movva NR, Hall MN. 1993. Target of rapamycin in yeast, TOR2, is an essential phosphatidylinositol kinase homolog required for G1 progression. *Cell* **73:** 585–596.

Lee SR, Collins K. 2005. Starvation-induced cleavage of the tRNA anticodon loop in *Tetrahymena thermophila*. *J Biol Chem* **280:** 42744–42749.

Letzring DP, Dean KM, Grayhack EJ. 2010. Control of translation efficiency in yeast by codon-anticodon interactions. *RNA* **16:** 2516–2528.

Loewith R, Jacinto E, Wullschleger S, Lorberg A, Crespo JL, Bonenfant D, Oppliger W, Jenoe P, Hall MN. 2002. Two TOR complexes, only one of which is rapamycin sensitive, have distinct roles in cell growth control. *Mol Cell* **10:** 457–468.

Miyake T, Reese J, Loch CM, Auble DT, Li R. 2004. Genome-wide analysis of ARS (autonomously replicating sequence) binding factor 1

(Abf1p)-mediated transcriptional regulation in *Saccharomyces cerevisiae*. *J Biol Chem* **279:** 34865–34872.

Motorin Y, Grosjean H. 1999. Multisite-specific tRNA:m^5C-methyltransferase (Trm4) in yeast *Saccharomyces cerevisiae*: Identification of the gene and substrate specificity of the enzyme. *RNA* **5:** 1105–1118.

Mushinski JF, Marini M. 1979. Tumor-associated phenylalanyl transfer RNA found in a wide spectrum of rat and mouse tumors but absent in normal adult, fetal, and regenerating tissues. *Cancer Res* **39:** 1253–1258.

Mushinski JF, Marini M. 1983. Tumor-specific tRNA modifications in mouse plasmacytomas and other tumors. *Recent Results Cancer Res* **84:** 121–132.

Natarajan K, Meyer MR, Jackson BM, Slade D, Roberts C, Hinnebusch AG, Marton MJ. 2001. Transcriptional profiling shows that Gcn4p is a master regulator of gene expression during amino acid starvation in yeast. *Mol Cell Biol* **21:** 4347–4368.

Owenby RK, Stulberg MP, Jacobson KB. 1979. Alteration of the Q family of transfer RNAs in adult *Drosophila melanogaster* as a function of age, nutrition, and genotype. *Mech Ageing Dev* **11:** 91–103.

Parsons AB, Brost RL, Ding H, Li Z, Zhang C, Sheikh B, Brown GW, Kane PM, Hughes TR, Boone C. 2004. Integration of chemical-genetic and genetic interaction data links bioactive compounds to cellular target pathways. *Nat Biotechnol* **22:** 62–69.

Pathak C, Jaiswal YK, Vinayak M. 2005. Hypomodification of transfer RNA in cancer with respect to queuosine. *RNA Biol* **2:** 143–148.

Phizicky EM, Hopper AK. 2010. tRNA biology charges to the front. *Genes Dev* **24:** 1832–1860.

Pintard L, Lecointe F, Bujnicki JM, Bonnerot C, Grosjean H, Lapeyre B. 2002. Trm7p catalyses the formation of two 2′-O-methylriboses in yeast tRNA anticodon loop. *EMBO J* **21:** 1811–1820.

Preston MA, Phizicky EM. 2010. The requirement for the highly conserved G_{-1} residue of *Saccharomyces cerevisiae* $tRNA^{His}$ can be circumvented by overexpression of $tRNA^{His}$ and its synthetase. *RNA* **16:** 1068–1077.

Randerath E, Agrawal HP, Randerath K. 1984. Specific lack of the hypermodified nucleoside, queuosine, in hepatoma mitochondrial aspartate transfer RNA and its possible biological significance. *Cancer Res* **44:** 1167–1171.

Reed SH, Akiyama M, Stillman B, Friedberg EC. 1999. Yeast autonomously replicating sequence binding factor is involved in nucleotide excision repair. *Genes Dev* **13:** 3052–3058.

Schaefer M, Pollex T, Hanna K, Tuorto F, Meusburger M, Helm M, Lyko F. 2010. RNA methylation by Dnmt2 protects transfer RNAs against stress-induced cleavage. *Genes Dev* **24:** 1590–1595.

Shaheen HH, Hopper AK. 2005. Retrograde movement of tRNAs from the cytoplasm to the nucleus in *Saccharomyces cerevisiae*. *Proc Natl Acad Sci* **102:** 11290–11295.

Sherman F. 1991. Getting started with yeast. *Methods Enzymol* **194:** 3–21.

Singhal RP, Vold B. 1976. Changes in transfer ribonucleic acids of *Bacillus subtilis* during different growth phases. *Nucleic Acids Res* **3:** 1249–1262.

Takano A, Endo T, Yoshihisa T. 2005. tRNA actively shuttles between the nucleus and cytosol in yeast. *Science* **309:** 140–142.

Thompson DM, Lu C, Green PJ, Parker R. 2008. tRNA cleavage is a conserved response to oxidative stress in eukaryotes. *RNA* **14:** 2095–2103.

Tomikawa C, Yokogawa T, Kanai T, Hori H. 2010. N7-Methylguanine at position 46 (m^7G46) in tRNA from *Thermus thermophilus* is required for cell viability at high temperatures through a tRNA modification network. *Nucleic Acids Res* **38:** 942–957.

Werner-Washburne M, Braun EL, Crawford ME, Peck VM. 1996. Stationary phase in *Saccharomyces cerevisiae*. *Mol Microbiol* **19:** 1159–1166.

Whipple JM, Lane EA, Chernyakov I, D'Silva S, Phizicky EM. 2011. The yeast rapid tRNA decay pathway primarily monitors the structural integrity of the acceptor and T-stems of mature tRNA. *Genes Dev* **25:** 1173–1184.

Whitney ML, Hurto RL, Shaheen HH, Hopper AK. 2007. Rapid and reversible nuclear accumulation of cytoplasmic tRNA in response to nutrient availability. *Mol Biol Cell* **18:** 2678–2686.

Wu P, Brockenbrough JS, Paddy MR, Aris JP. 1998. *NCL1*, a novel gene for a non-essential nuclear protein in *Saccharomyces cerevisiae*. *Gene* **220:** 109–117.

Ye Y, Meyer HH, Rapoport TA. 2001. The AAA ATPase Cdc48/p97 and its partners transport proteins from the ER into the cytosol. *Nature* **414:** 652–656.

Yoshikawa K, Tanaka T, Ida Y, Furusawa C, Hirasawa T, Shimizu H. 2011. Comprehensive phenotypic analysis of single-gene deletion and overexpression strains of *Saccharomyces cerevisiae*. *Yeast* **28:** 349–361.

Zaborske JM, Narasimhan J, Jiang L, Wek SA, Dittmar KA, Freimoser F, Pan T, Wek RC. 2009. Genome-wide analysis of tRNA charging and activation of the eIF2 kinase Gcn2p. *J Biol Chem* **284:** 25254–25267.